

PERFORMANCE OF OTR AND SCINTILLATOR VIEW SCREENS FOR THE ARIEL ELECTRON LINAC

D.W. Storey^{†,1,2}, J.M. Abernathy¹, D. Karlen¹, M. Pflieger¹, P. Poffenberger¹, P. Birney², P.E. Dirksen², S.R. Koscielniak², M. Lenckowski²

¹University of Victoria, Victoria, Canada, ²TRIUMF, Vancouver, Canada

Abstract

The ARIEL electron linac is a 0.3MW CW accelerator, extensible to 0.5 MW, being installed at TRIUMF for radioactive beam production. To date, 17 view screen monitors have been installed along the beamline and have proven to be essential tools in the commissioning of e-linac systems. These are populated by two types of beam targets: P46 scintillator screens which provide diagnostics for low duty factor operation, while at locations with beam energies at and above 10 MeV, OTR foils using either Pyrolytic Graphite or Niobium foils are included to provide coverage up to 100's of μA average beam current. The design of the view screen is described including the image acquisition system and beam target selection. The performance thus far of the OTR foils under low duty factor commissioning is presented including quantification of the OTR emission distribution, thermal studies, and transmission of the beam through the linac after intercepting a foil.

INTRODUCTION

The transverse beam profile is measured along the ARIEL electron linac (e-Linac) [1] by view screens, wire scanners, and at low energy, slit scanners. The view screen systems are intercepting devices that provide real-time 2D images of the transverse beam profile by inserting a target into the beamline that produces light when the beam passes through, and imaging the resulting distribution. 17 view screen systems are installed along the beamline with more planned in the remaining ~ 50 m of transport beam line to the ARIEL target stations.

DESIGN

Each view screen contains a number of optical targets mounted on a target ladder that may be actuated into the beamline or retracted when not in use. Each system is outfitted with an optical calibration target with a pattern of holes spaced on a grid to provide both geometric calibration and to correct for distortions introduced by the imaging optics. For use at low beam currents, P46 phosphor scintillator screens are included in most stations. Optical Transition Radiation (OTR) targets are included in view screens installed where the nominal beam energy is 10 MeV or greater. The use of both target types provides a wide dynamic range of the system, allowing visibility from nA beams with the scintillator foil up to 100's of μA average beam current with the OTR foils.

The targets are oriented at 45° with respect to beam axis allowing the light produced to pass through a fused

silica view port window for image acquisition. A mirror in the optical path reflects the visible light upwards 90° to allow the optical elements to be placed out of line of sight of the beamline to reduce radiation damage. The light is focused through a pair of achromatic doublet lenses onto a 12 bit GigE CCD camera for imaging. Two different optics designs are used to achieve fixed 50 mm and 25 mm fields of view for cameras located in the low energy ($<300\text{keV}$) or higher energy beamlines respectively. The cameras are mounted tilted with respect to the optics axis to allow the camera to focus across the entire rotated beam target. This configuration is shown in Figure 1.

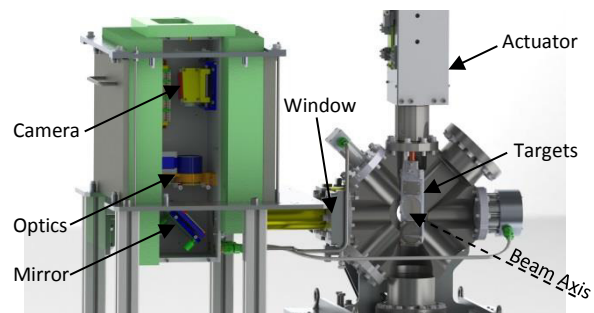


Figure 1: The view screen system installed on the beamline showing the target ladder and imaging system.

Beam Target Selection

The initial selection for the scintillation screens was single crystal YAG:Ce due to its thermal and scintillation properties. However, in initial low energy beam tests with a 60 keV beam the targets were found to accumulate electric charge due to the insulating properties of the YAG:Ce leading to distortions to the beam profile as the beam was repelled by the charged target surface and eventually damage to the target surface when then the target discharged. To overcome this issue of charging, the YAG:Ce targets were initially coated with a 10 nm layer of gold to aid in grounding the targets. For the production units, the scintillator targets were replaced with ultra-fine ($2\ \mu\text{m}$ grain) P46 phosphor on 0.2 mm aluminium backing from TMS Vacuum Components.

For OTR targets, both $25\ \mu\text{m}$ niobium (Nb) and $8\ \mu\text{m}$ Pyrolytic Graphite (PG) foils have been installed at different locations along the linac. The selection of foil material was guided by thermal and optical properties, as well as their interaction properties with the beam. In addition to PG and Nb, titanium, stainless steel and aluminium foils were considered.

The thermal response of the targets was determined using the energy deposited in the 0.1 mm minimum spot sizes from the different target materials using the ESTAR

[†]dstorey@triumf.ca

database of stopping powers for electrons [2]. PG has a very high thermal conductivity in the plane of the foil and therefore can take several 100 μA beam current before reaching 500°C, after which thermal radiation could start interfering with image acquisition. Nb, Ti, and SS foils all reach >100°C at beam currents of 10's of μA due to their lower thermal conductivities and higher density (more energy loss by the beam). Only Al performs similarly to PG, however with a melting temperature of 660°C, would have a much reduced peak beam current.

Beam scattering after passing through the foils is also of concern for limiting beam loss downstream of an intercepting OTR foil. The scattering can be approximated by the Molière scattering distribution, which provides the RMS width of the Gaussian distributed scattering angles from the beam energy and material's radiation length. Again PG has optimal properties here due to its low density compared to the metal foils.

The beam loss caused by beam scattering can be estimated by calculating the fraction of electrons scattered outside of a reasonable acceptance angle. For a 10 MeV beam and assuming an acceptance angle of around 20 mrad, around 2% of the beam would be lost after the PG foils, whereas about 98% is lost after a 25 μm Nb foil.

The light output by the OTR process is dependent on the permittivity of the material, ϵ_r , and approximately scales with the reflectivity:

$$R = \left| \frac{\sqrt{\epsilon_r} - 1}{\sqrt{\epsilon_r} + 1} \right|^2 \quad (1)$$

In the visible spectrum, the reflectivity of PG was estimated to be ~0.3, and is relatively low compared to metallic foils. The reflectivity of Nb is 0.5, and aluminium is even higher at around 0.9.

Overall, PG was determined to be the optimal target material as it results in the lowest amount of beam scattering, energy loss to beam, and the lowest resulting target temperatures. This allows the PG OTR foils to be used at beam current up to 100's of μA of average beam current. The 50 mm, 8 μm thick PG foils were sourced from Minteq Pyrogenics Group. Several Nb foils have also been installed in the beamline.

Foil Mounting

The PG foils are mounted under tension to provide a flat surface for the production of light by OTR. The foils are mounted between two rings made from bulk PG to match the thermal expansion coefficient of the foil. The two rings have matching ridge and groove features on their mating faces which catch the foil as they are being clamped together and pull uniformly around the circumference of the foil to tension the foil like a drum head. A few iterations of the ridge and groove dimensions were tested to provide adequate tension of the mounted foil without tearing the foil. Figure 2 shows a schematic of the two halves of the mounting ring and the foil after tensioning. The robustness of this mounting was tested by applying repeated thermal cycling to a mounted foil, applying air pressure to one side of the foil, and pressing

on the centre of the foil, with the foil surviving all reasonable test situations.

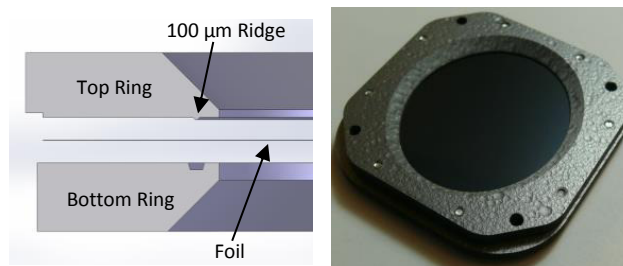


Figure 2: The ridge and groove mounting assembly, showing a mounted PG foil on the right. The mounting rings are flat and smooth, despite the appearance.

OTR TARGET BEAM TESTS

Commissioning of the OTR view screen systems was performed in the 10-MeV section of the e-Linac which had four Nb foils and one PG foil installed. Commissioning studies were limited to 100 W average beam power as the machine protection system was not fully in place at the time.

An initial test was performed to check for consistency between images captured by scintillator target and OTR screen. Figure 3 shows a profile captured under the same conditions with either target, showing good agreement between the two types of targets. The scintillator screen produces approximately 2000 times more light than the PG OTR target, requiring a 20 dB gain to be applied to the OTR to allow it to be visible under the same beam conditions.

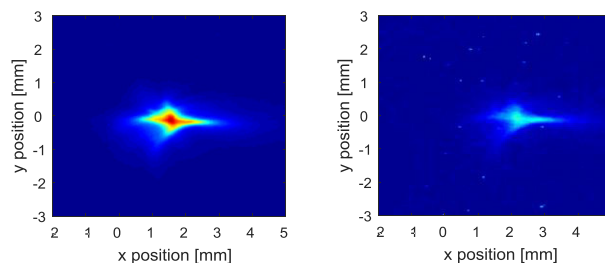


Figure 3: The beam profile from the P46 scintillation target (left) and PG OTR foil (right) imaged from the same view screen system.

In the range of 10 – 50 MeV, OTR light is emitted primarily in two lobes around the reflection axis from the foil with respect to the beam axis. These lobes are peaked at an angle of $\sim \pm 1/\gamma$ from the reflection axis where γ is the Lorentz factor. The OTR emission distribution is described in [3]. A sketch of this emission distribution, in relation to the optics setup is shown in Figure 4.

Tests were performed to compare the light produced by the foils to this theoretical distribution. Beam profile images were measured under different beam conditions with the image intensity determined by fitting a 2D Gaussian distribution to the acquired profile images. The expected image intensity was determined using a MATLAB script to integrate the OTR emission distribu-

tion over the aperture of the camera using the fitted beam parameters and the frequency response of the camera. For images acquired using the PG foils, the acquired image intensity is on average 40% lower than the expected intensity. This could be explained by non-perfect transmission through the optics, overestimating the charge contained in non-Gaussian beam tails, or other uncertainties in misalignment, beam energy, etc. Fewer statistics were acquired using the Nb foils, but they were found to show a similar light output as the PG foils, rather than the roughly 70% more light due their higher reflectivity.

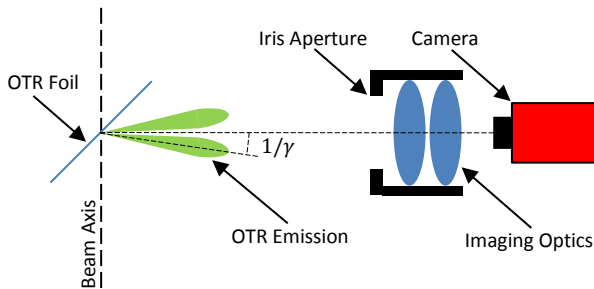


Figure 4: A schematic of the OTR emission distribution relative to the imaging optics (not to scale).

The light imaged was confirmed to be OTR light and not thermally emitted blackbody radiation by analysing the image intensity with increasing average beam currents. The acquired image intensities were found to increase linearly with beam current, whereas thermal emission would be expected to increase much more rapidly with temperature (and thus beam current). No evidence of thermal radiation interfering with OTR was found, up to the few μA average currents measured.

The non-uniform angular emission distribution of OTR allowed for further studies to quantify this distribution by changing the angular acceptance of the camera to capture different regions of the emission distribution. This was done first by scanning the imaging system’s iris aperture with a stable beam profile. The extracted image intensity agrees very well with expected intensity due to the OTR emission distribution, as seen in Figure 5.

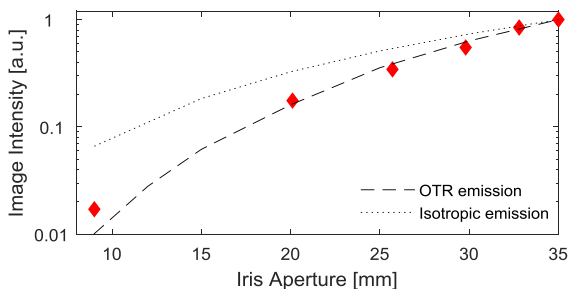


Figure 5: OTR image intensity (♦) with changing iris aperture compared to the expected intensity from the OTR emission distribution or isotropic emission.

To further probe the OTR emission distribution, images were acquired of the beam as it was scanned horizontally and vertically by an amount small enough to preserve the beam shape. Changing the position of the

beam on the OTR foil changes the fraction of the emission distribution captured by the imaging system. This was performed with two iris settings with good agreement, with the more noticeable effect seen with the iris closed very small, as expected, Figure 6.

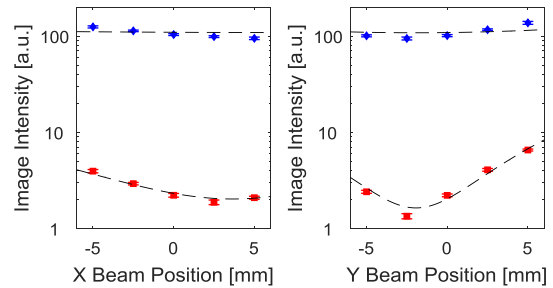


Figure 6: OTR image intensity with the beam scanned in horizontal (left) and vertical (right) directions across the screen, with the iris open (♦), and closed (■). The dashed lines show the comparison to expected image intensity.

Finally, the transmission of the beam through the foils to a downstream location was determined by measuring the beam current in a downstream Faraday cup with and without the OTR foils in place. After passing through a PG foil, 93% of the original beam current was measured at the downstream location, while inserting a Nb foil resulted in only a 4% transmission. The beam was not returned between these measurements and the two foils measured were separated by ~ 1 m, but still confirms the expected effect on the beam of the two types of foils. This indicates that commissioning that is completed with the Nb OTR foils is limited to low beam powers due to the fact that almost the entire beam will be lost on the downstream beam pipe.

CONCLUSION

The view screen systems have proven to be an important tool in commissioning studies with both OTR and scintillation screens operating as designed. Further commissioning of the view screen systems is planned with beam energies up to 30 MeV and beam power above 100 W. Another 8 view screen systems in e-Linac will be outfitted with PG OTR targets in the near future.

ACKNOWLEDGMENT

The authors would like to thank Brandon Humphries, Eric Chapman, and Ryan Lovelidge for operating the e-Linac during these measurements. The author’s travel to IPAC’17 has been supported by the Division of Physics of the United States National Science Foundation (Accelerator Science Program) and the Division of Beam Physics of the American Physical Society.

REFERENCES

- [1] S.R. Koscielniak *et al.*, in *Proc. IPAC’17*, TUPAB022, 2017.
- [2] NIST, *ESTAR: Stopping power and range tables for electrons*, <http://physics.nist.gov/PhysRefData/Star/Text/ESTAR.html>
- [3] D. Giove *et al.*, in *Proc PAC’95*, TPC10, 1995.